Computational Insight into Anti-mutagenic Properties of CYP1A Flavonoid Ligands

Rute da Fonseca[&], Michele Marini[‡], André Melo[&], Maria Cristina Menziani[‡] and Maria João Ramos*[,&]

[&]*Departamento de Química, Faculdade de Ciências, Universidade do Porto, Rua do Campo Alegre, 687, 4169-007 Porto, Portugal and* [‡]*Dipartamento di Chimica, Università di Modena and Reggio E., Via Campi 183, 41100 Modena, Italy*

Abstract: Cytochrome P450 1A (CYP1A) is a subclass of enzymes involved in the biotransformation of heterocyclic amines present in cooked red meat to carcinogenic compounds. Anti-cancer properties have long been associated with flavonoids, and some compounds of this class have been shown to interact directly with CYP1A2. The understanding of this interaction is the purpose of this work. As the number of experimentally tested molecules is limited, two complementary methods in terms of information provided, are proposed for the study of protein-inhibitor interaction as alternatives to a QSAR analysis, using quantum mechanics as well as molecular mechanics.

Key Words: Binding free energy, cancer, CYP1A2, cytochrome P450, flavonoids, molecular mechanics, quantum mechanics.

INTRODUCTION

Cytochrome P450 (CYP) is a large class of enzymes which represents 12% of all the human cytochrome. These enzymes are responsible for transforming xenobiotic substances into products easier to remove from the body. Other important roles of CYPs are the synthesis of steroid hormones thromboxane, cholesterol and bile acid and the degradation of endogenous compounds such as fatty acids, retinoic acids and steroids [1].

Despite the benefits of their actions, CYPs also produce toxins and mutagenic compounds. For example, some heterocyclic amines (HAs), which can be found in significant amounts in meat cooked at high temperatures, are N-hydroxylated by CYP class 1A enzymes (CYP1A) to toxic mutagens. These compounds can cause DNA damage, which results in the formation of tumors in a variety of tissues in several species [2-4]. Flavonoids reduce the risk of DNA damage by competing with the HAs for binding to the CYP1A active site [5-10], and therefore inhibiting its damaging catalytic activity.

CYPs are involved in interactions with flavonoid compounds in at least three ways: (i) flavonoids induce the biosynthesis of several CYPs; (ii) enzymatic activities of CYPs are modulated (inhibited or stimulated) by these compounds; and (iii) flavonoids are metabolized by several CYPs [9].

In humans, the CYP1A inhibition mechanism by flavonoids is very complex, involving a large number of chemical and biological aspects. For a detailed description of such mechanism, it is essential to understand the molecular recognition of flavonoids by CYP1A at molecular level.

*Address correspondence to this author at the Departamento de Química, Faculdade de Ciências, Universidade do Porto, Rua do Campo Alegre, 687, 4169-007 Porto, Portugal; E-mail: mjramos@fc.up.pt

We have carried out a theoretical study of the anti-mutagenic properties of 8–Prenylnaringenin (8-PN), Isoxanthohumol (IX) and Xanthohumol (XN) (see Fig. (**1**)). These compounds occur naturally in hops and beer and their inhibitory power towards human CYP1A2 (hCYP1A2) metabolism has been tested experimentally [11]. Using this data, it is possible to make both a qualitative and semi-quantitative evaluation of the ligands inhibitory potency based on structural data. By analyzing the electrostatic potential of all the ligands, we can indicate which features are most likely to be related to a higher inhibitory power, either because these are involved in molecular recognition processes or in stabilization at the active site.

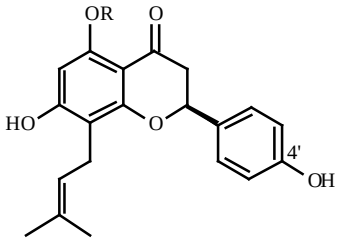

R = H for 8-Prenylnaringenin (**8-PN**)
R = CH_3 for Isoxanthohumol (**IX**)

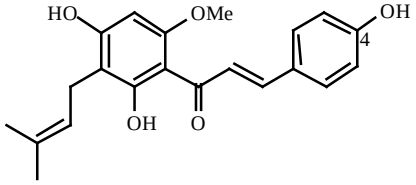

Xanthohumol (**XN**)

Fig. (1). Flavonoids used in this study.

1573-4064/05 $50.00+.00

This last characteristic can be further explored by the assessment of the interaction energy between specific residues in the active site and the ligand obtained by means of enzyme-ligand complex calculations [12,13]. Actually, it is possible to compare the affinities of different ligands towards the same enzyme by calculating appropriated thermodynamic quantities. In this work, two approaches have been used to correlate the inhibitory power determined experimentally with calculated properties, using both explicit and continuum descriptions of the solvent.

MATERIALS AND METHODS

The ligands' structures were modeled using InsightII [14]. The S diastereoisomer conformation on carbon 2 was used for 8-PN and IX; this is the diastereoisomer naturally occurring in hops [15].

Molecular Electrostatic Potentials

The ligands were then minimized at the B3LYP/6-31G* level, using Gaussian98 [16]. The molecular electrostatic potentials for the optimized geometries have been generated using the CUBEGEN utility available in Gaussian98 [16]. The molecular electrostatic potential (values ranging from –56 kcal/mol to 56 kcal/mol) was mapped onto 0.002 e/bohr^3 electron density surface with Molekel 4.2 [17].

Dockings

The ligands were docked onto the active site of hCYP1A2 [12], using GOLD [18]. GOLD provides two scoring functions for analyzing the results of a search for the best binding of a ligand (allowing its total conformational flexibility) in an active site cavity by using a genetic algorithm: GoldScore, the original scoring function, optimized for predicting ligand binding positions, and ChemScore, derived from regression against ligand-receptor binding free energies [18]. We have used both of these scoring functions and the standard default settings, to get the best 5 results of 50 docking runs for each ligand. In order to get a reliable orientation, we have used a distance constraint of 5 Å between the heme's iron and the oxygen on carbon C4' in 8-PN and IX, and the correspondent carbon C4 in XN, as this seems to be the potential site of oxidation of flavonoid type structures by members of the cytochrome P450 family [19,20]. Visualization of docking results was performed with DS ViewerLite from Accelrys [14].

Stabilization Energies of Complexes

The best results of the docking were then energy minimized using CHARMM27 [21]. We have used the complete model solvated with a 9 Å layer of TIP3P explicit water molecules. Several steps of minimization have been done. First, the docking position of the ligand has been optimized together with the side-chains of the aminoacids. Next, the backbone of the enzyme was relaxed, with harmonic constrains of 2 kcal.mol^{-1} on the residues located more than 20 Å away from the ligand. In all steps, harmonic constraints have been applied to the water molecules, which are located between 6 and 9 Å away from the enzyme, to prevent the solvent from evaporating. The ligands were also geometrially optimized inside a 20 Å sphere of TIP3P explicit water molecules. Harmonic constraints have been applied to the water molecules, which are located more than 15 Å away from the centroid of the system, resulting in the same number of constrained molecules for the three ligand-water complexes.

Using the structures solvated with water molecules, the hCYP1A2/flavonoids complexes stabilization energy, $\Delta E_{aq}^{stab}(E:L)$, has been calculated as follows:

$$\Delta E_{aq}^{stab}(E:L) = E_{aq}(E:L) - E_{aq}(E) - E_{aq}(L) \quad (1)$$

$E_{aq}(E)$ is the energy of the isolated solvated enzyme, and $E_{aq}(L)$ is the energy of the isolated solvated flavonoid. Within a molecular mechanics formalism, the stabilization energy can be partitioned as

$$\Delta E_{aq}^{stab}(E:L) = \Delta E_{\text{int}}(E:L) + \Delta E_{conf}(E:L) + \Delta E_{solv}(E:L) \quad (2)$$

where is $\Delta E_{\text{int}}(E:L)$ interaction energy between the enzyme and the flavonoid within the hCYP1A2:flavonoid complex, and $\Delta E_{conf}(E:L)$ corresponds to the energy needed to change the conformation of the enzyme and ligand from the free to the complexed form. $\Delta E_{solv}(E:L)$ is the difference in energy correspondent to the interactions with the solvent between the free and the complexed form of both enzyme and ligands.

In this work, the most significant specific interfragment interactions responsible for the stabilization for the hCYP1A2/flavonoid complexes have been evaluated using the INTER utility available in CHARMM27 [21].

Binding Free Energies of the Complexes

The binding free energy of the same complexes calculated, combining the use of molecular mechanics and a classical continuum solvation approach. The binding free energy can be defined as [22]:

$$\Delta G_{bind} = G_{aq}(E:L) - \left[G_{aq}(E) + G_{aq}(L)\right] \quad (3)$$

where $G_{aq}(E:L)$, $G_{aq}(E)$ and $G_{aq}(L)$ correspond to Gibbs free energies. The Gibbs free energy of a generic species is [22]:

$$G_{aq} = G_{gas} + G_{solv} \quad (4)$$

In equation [4], G_{gas} is the binding free energy of the species in gas phase and G_{solv} is its solvation free energy. G_{gas} corresponds to the sum of the energy of the species in gas phase ($E_{gas} = \Delta E_{\text{int}}(E:L) + \Delta E_{conf}(E:L)$) with the correspondent entropic contribution. The latter can be regarded as non-differential when comparing two complexes, as it refers to the process of association of similar ligands to the same protein [22,23] and will not be considered. The solvation entropic effects are included in the continuum method used to solvate our systems.

G_{solv} can be partitioned into polar and non-polar terms:

$$G_{solv} = G_{solv}^{polar} + G_{solv}^{nonpolar} \quad (5)$$

The polar solvation free energy was calculated by solving the Poisson-Boltzmann equation with the Delphi program [24]. The nonpolar component was calculated using the solvent accessible surface area as follows [25]:

$$\Delta G_{solv}^{nonpolar} = \gamma A + b \quad (6)$$

where A is the solvent accessible surface area of the species calculated in InsightII [14] using a 1.4 Å radius probe. γ and *b* are 0.00542 kcal.mol^{-1} and 0.92 kcal.mol^{-1}, respectively [25].

All the energy values will be presented as normalized with respect to the weakest ligand, XN.

RESULTS AND DISCUSSION

In this study, we present different approaches to the ligand binding efficiency prediction, when the number of molecules tested experimentally is too small for a QSAR type of study.

The experimental inhibitory activity data available measures the degree of inhibition of the mutagenesis of 2-amino-3-methylimidazo-[4,5-f]quinoline (IQ) in a Salmonella Assay induced by a concentration of 10μM of flavonoid. The experimental data was obtained by *in vitro* analysis with human DNA recombinant CYP1A2, guaranteeing the absence of interference of other enzymes in the process [11].

A first step towards the understanding at molecular level of the experimental results was the characterization of the molecular electrostatic recognition pattern of the flavonoids. These represent the electrostatic potential profile of the ligand, which allows the identification of enzyme-ligand interaction sites based on the concept of electrostatic complementarity. These interactions may be important as molecular recognition features when the ligand approaches the enzyme, and for electrostatic complementarities between the docked ligand and the active site.

The optimized geometries of the ligands obtained at B3LYP/6-31G* level are presented in Fig. (**2**), together with the respective molecular electrostatic potentials mapped onto an electron density surface. It can be observed that all the flavonoids present common patterns in the electrostatic potential surface. In fact, the most negative potentials are located on the oxygen atoms of carbonyl, hydroxyl and methoxy groups. These will be hydrogen bonding spots, as can be seen in Fig. (**3**), which will stabilize the ligands in the complex (see Table **1**). One marked difference between the two best inhibitors and XN is the presence of strong negative potential spots all around the molecule in the latter, while for the first two, these spots are located only in one side, which is the upper side in Fig. (**2**). This will be important because the lower side will be facing Phe_{125}, which shows a highly stabilizing van der Waals interaction with the ligands (the van der Waals term represents over 90% of the total interaction energy for this residue).

Next, an appropriate docking of the inhibitors into the active site using an automated approach was done, followed by a geometry optimization of the complexes using molecular mechanics. The results of this procedure were used in two ways with the aim of relating the experimentally determined inhibitory power of the flavonoids with an appropriate thermodynamic quantity. One of them implies the use of explicit water molecules to solvate ligand and enzyme. This procedure enables the description of interactions for individual atoms or sets of atoms. A detailed description of the specific interactions responsible for the stability of the enzyme-inhibitor complexes has been carried out with the aim of designing possible anti-mutagenic compounds in future works. Using this approach, the stabilization energy of the complexes was calculated, based on the molecular mechanics energy obtained for the solvated

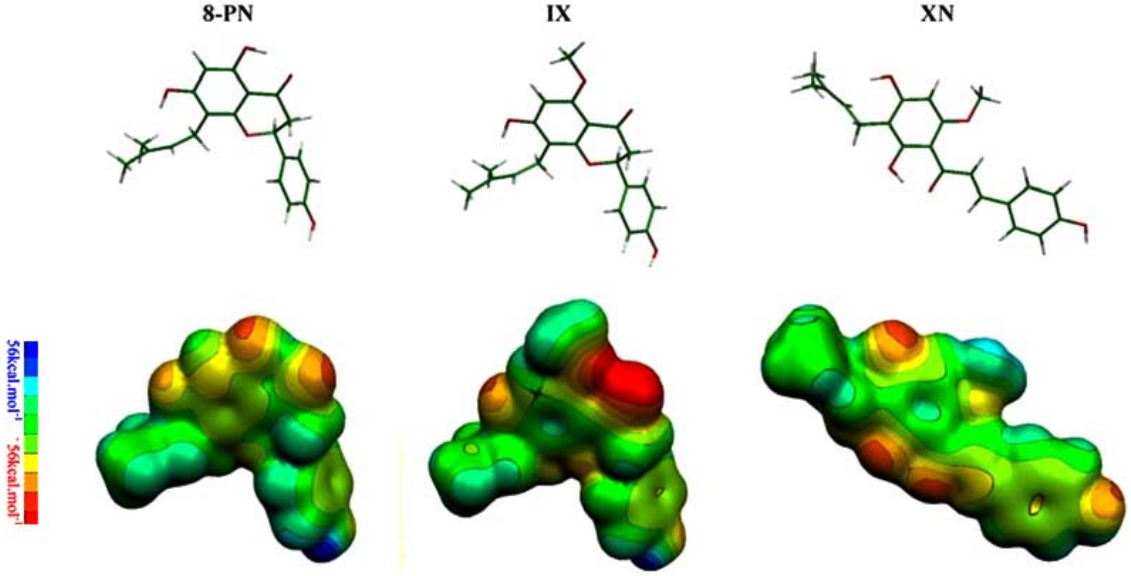

Fig. (2). 8-PN, IX and XN after geometry optimization with DTF using B3LYP with the 6-31G* basis set and their MEPs mapped onto a 0.002e/borh3 electron density surface.

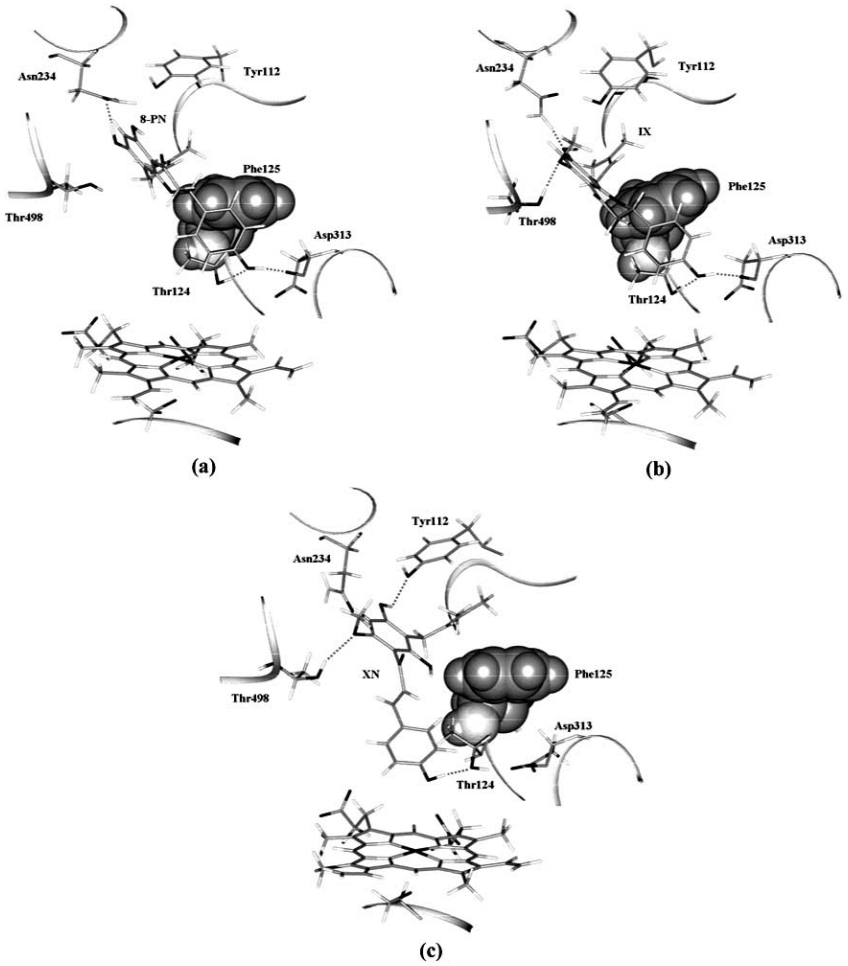

Fig. (3). Active site of the hCYP1A2/flavonoid complexes (a) with 8-PN, (b) IX and (c) XN after geometry optimization. The residues which present the most significant interaction energies with the ligands (see Table **1**) are shown. Hydrogen bonding is indicated by grey lines.

complexes and ligands. This quantity was well correlated with the experimentally determined inhibitory power of the flavonoids. The main interactions of the complexes can be analyzed using the decomposition of $E_{\text{int}}(E:L)$ into the appropriate components (Table **1**).

Considering the interactions between the flavonoids and the residues of hCYP1A2, it can be observed that all three flavonoids share a large number of specific interactions (Tyr_{112}, Thr_{124}, Phe_{125}, Asp_{313}, Asn_{234} and Thr_{498}, see Table **1**). These interactions represent 50% of the total interaction energy between the flavonoids and the rest of the system ($E_{\text{int}}(E:L)$). Additionally, the interactions involving Val_{227}, Ala_{230}, Ser_{231}, Ile_{386}, Leu_{497} have Met_{499} have a significant role in the stabilization of the complexes, representing around 20% of the total $E_{\text{int}}(E:L)$. A very strong interaction common to the three ligands corresponds to a hydrogen bond between the side chain of Thr_{124}, deeply buried in the active site and the hydroxyl substituent in carbon C4 for 8-PN and IX or carbon C4' in XN (see Fig. (**3**)). This substituent is further stabilized with an interaction with the oxo group from the backbone of Asp_{313} in 8-PN and IX. This interaction is not present for the complex with XN, and instead, this compound presents the highest single aminoacid interaction energy contribution to $E_{\text{int}}(E:L)$, with a residue located at the entrance of the active site, Thr_{498}.

Moreover, XN is disfavored in relation to the other two, for an already mentioned strong stabilizing interaction with Phe_{125}, common to all the ligands. The ligands structure is wrapped around the side-chain of this residue, with the prenyl substituent almost parallel to one side of the aromatic ring and the phenyl substituent coming down to the other face of the ring (see Fig. (**3**)), towards the interaction with Thr_{124} and Asp_{313}. Although the fit of XN in the active site leads to a higher total $E_{\text{int}}(E:L)$ (see Table **2**), this does not necessarily imply a higher stabilization of this ligand inside the enzyme. Stabilizing interactions that are related to a higher residence time such as those with the residues buried in the cavity Thr_{124} and Asp_{313}, or the anchor-like effect of the interaction with Phe_{125}, are less important to the total $E_{\text{int}}(E:L)$ when compared to the other two ligands.

Another disadvantageous property of the complex between hCYP1A2 and XN is the high energy cost of the conformational changes that both ligand and enzyme undergo to form the complex when compared to the other two (see Table **2**). This component of the stabilization energy of the hCYP1A2/flavonoid complexes is correlated

Table 1. Most Significant Interaction Energies (in Bold, >5kcal.mol^{-1}) Between Individual Residues of the Human CYP1A2 Active Site and 8-PN, IX and XN

	8-PN		IX		XN	
Aminoacid residue	E_{int} (kcal.mol^{-1})	Interaction	E_{int} (kcal.mol^{-1})	Interaction	E_{int} (kcal.mol^{-1})	Interaction
Tyr 112	**-5.0**	3,5A electrostatic interaction	**-5.4**	3A electrostatic interaction	**-6.3**	H-bond
Thr 124	**-6.3**	H-bond	**-10.0**	H-bond	**-10.5**	H-bond
Phe 125	**-5.0**	Ligand folds around its side-chain	**-5.8**	Ligand folds around its side-chain	-3.1	Ligand folds around its side-chain
Asn 234	**-10.5**	H-bond	**-5.5**	H-bond	-2.2	
Asp 313	**-8.5**	H-bond	**-7.4**	H-bond	-3.8	
Thr 498	-1.4		**-7.8**	H-bond	**-14.6**	H-bond

with the experimentally determined inhibitory activities, and will be determinant for the overall stabilization of the complex. The large methoxy group that distinguishes structure IX from the best inhibitor's will be responsible for its lower inhibitory power because of the enzyme's conformational rearrangement term, although it actually contributes to a docking position that provides an extra stabilizing hydrogen bond interaction when compared to 8-PN (see Fig. (**3**)). XN is disfavored in all stabilization energy components.

The second method described here deals with the solvent as a continuum. In this case, it is possible to calculate the binding free-energy of the complexes, and this was also correlated with the inhibitory power of the flavonoids. There was a full agreement between the relative $\Delta G_{bind}(E:L)$ and the experimental inhibition results (see Table **3**).

These values were strongly dependent on the gas phase energy component. In fact, $\Delta G_{solv}(E:L)$ actually favored XN in relation to the other ligands, but $\Delta E_{gas}(E:L)$ was decisive for the final $\Delta\Delta G_{bind}(E:L)$ value.

CONCLUSION

We have presented two different approaches complementary in terms of information provided, to study the ligand binding problem. One used an atomistic description of the solvent, and allowed us to calculate the stabilization energy of the complexes. The other includes the use of continuum methods in a classical approach, allowing us to calculate the correspondent binding free-energies. Both correlated with the experimental results for inhibition of hCYP1A2. The inhibitory power is strongly correlated with the conformational rearrangement energies. There are also some specific structural features of the ligands contributing to a higher binding energy. One is the presence of small electronegative groups bound to the atoms that sit between C8 and the oxo group of flavanone-like structures which participate in stabilizing hydrogen bond type interactions with Tyr_{112}, Asn_{234} and Thr_{498}. The prenyl tail in the compounds helped stabilizing the complex through non-polar interactions with Phe_{125}, which seems to be an important residue in the fitting of the ligands in the active site. The hydroxyl substituent in C4 in 8-PN and IX, or carbon C4' in XN should contribute for a longer residence time, as it is involved in hydrogen bonding with residues which are buried in the active site, Thr_{124} and Asp_{313}.

It is a noteworthy fact that the flavonoids studied establish strong stabilizing interactions with both Thr_{124} and

Table 2. Stabilization Energy of the Complexes Between Human CYP1A2 and 8-PN, IX and XN. All the Values are Normalized with Respect to the Weakest Ligand, XN

hCYP1A2 complex	**%inhibition**	$\Delta\Delta E_{int}(E:L)$ **(kcal.mol^{-1})**	$\Delta\Delta E_{conf}(E:L)$ **(kcal.mol^{-1})**	$\Delta\Delta E_{solv}(E:L)$ **(kcal.mol^{-1})**	$\Delta\Delta E_{stab}(E:L)$ **(kcal.mol^{-1})**
8-PN	94	6.6	-132.1	-416.4	-541.9
IX	84	1.1	-110.2	-211.3	-320.3
XN	48	0	0	0	0

Table 3. Binding Free Energies of the Complexes Between Human CYP1A2 and 8-PN, IX and XN. All the Values are Normalized with Respect to the Weakest Ligand, XN

hCYP1A2 complex	%inhibition	$\Delta\Delta E_{gas}(E:L)$ (kcal.mol^{-1})	$\Delta\Delta G_{solv}(E:L)$ (kcal.mol^{-1})	$\Delta\Delta G_{bind}(E:L)$ (kcal.mol^{-1})
8-PN	94	-125.6	69.4	-56.1
IX	84	-109.0	96.8	-12.2
XN	48	0	0	0

Val_{227}, which have been shown to be important for the maintenance of the catalytic activity of hCYP1A2 [26,27]. This constitutes an extra validation of the results obtained in the present work.

ACKNOWLEDGEMENTS

We thank the FCT (Fundação para a Ciência e Tecnologia) for a doctoral scholarship for R.F. and the NFCR (National Foundation for Cancer Research) Centre for Drug Discovery, University of Oxford, U.K., for financial support. M.M. was supported by a bilateral Erasmus agreement.

REFERENCE

[1] Guengerich, F. P. *Chem. Res. Toxicol*., **2001**, *14*, 611.
[2] Boobis, A. R.; Lynch, A. M.; Murray, S.; de la Torre, R.; Solans, A.; Farre, M.; Segura, J.; Gooderham, N. J.; Davies, D. S. *Cancer Res*., **1994**, *54*, 89.
[3] Turesky, R. J.; Constable, A.; Richoz, J.; Varga, N.; Markovic, J.; Martin, M. V.; Guengerich, F. P. *Chem Res Toxicol*., **1998**, *11*, 925.
[4] Garner, R. C.; Lightfoot, T. J.; Cupid, B. C.; Russell, D.; Coxhead, J. M.; Kutschera, W.; Priller, A.; Rom, W.; Steier, P.; Alexander, D. J.; Leveson, S. H.; Dingley, K. H.; Mauthe, R. J.; Turteltaub, K. W. *Cancer Lett*., **1999**, *143*, 161.
[5] Zhai, S.; Dai, R. K.; Friedman, F. K.; Vestal, R. E. *Drug Metab. Dispos*., **1998**, *26*, 989.
[6] Zhai, S.; Dai, R.; Wei, X.; Friedman, F. K.; Vestal, R. E. *Life Sci*., **1998**, *63*, 119.
[7] Bear, W. L.; Teel, R. W. *Anticancer Res.*, **2000**, *20*, 3609.
[8] Hodek, P.; Trefil, P.; Stiborová, M. *Chemico-Biological Interactions*, **2002**, *139*, 1.
[9] Lee, H.; Yeom, H.; Kim, Y. G.; Yoon, C. N.; Jin, C.; Choi, J. S.; Kim, B. R.; Kim, D. H. *Biochem. Pharmacol*., **1998**, *55*, 1369.
[10] Edenharder, R.; Rauscher, R.; Platt, K. L. *Mutat. Res*., **1997**, *379*, 21.
[11] Miranda, C. L.; Yang, Y. H.; Henderson, M. C.; Stevens, J. F.; Santana-Rios, G.; Deinzer, M. L.; Buhler, D. R. *Drug Metab. Dispos*., **2000**, *28*, 1297.

Received: 01 December, 2004 Accepted: 10 March, 2005

[12] Fonseca, R.; Menziani, M. C.; Melo, A.; Ramos, M. J. *Molecular Physics*, **2003**, *101*, 2731.
[13] De Rienzo, F.; Fanelli, F.; Menziani, M. C.; De Benedetti, P. G. *J. Comput. Aided Mol. Des*., **2000**, *14*, 93.
[14] http://www.accelrys.com .
[15] Heller, W. *Acta Horticulturae*, **1994**, *381*, 46.
[16] Frisch, M. J.; Trucks, G. W.; Schlegel, H. B.; Scuseria, G. E.; Robb, M. A.; Cheeseman, J. R.; Zakrzewski, V. G.; Montgomery Jr, J. A.; Stratmann, R. E.; Burant, J. C.; Dapprich, S.; Millam, J. M.; Daniels, A. D.; Kudin, K. N.; Strain, M. C.; Farkas, O.; Tomasi, J.; Barone, V.; Cossi, M.; Cammi, R.; Mennucci, B.; Pomelli, C.; Adamo, C.; Clifford, S.; Ochterski, J.; Petersson, G. A.; Ayala, P. Y.; Cui, Q.; Morokuma, K.; Rega, N.; Salvador, P.; Dannenberg, J. J.; Malick, D. K.; Rabuck, A. D.; Raghavachari, K.; Foresman, J. B.; Cioslowski, J.; Ortiz, J. V.; Baboul, A. G.; Stefanov, B. B.; Liu, G.; Liashenko, A.; Keith, T.; Al-Laham, M. A.; Peng, C. Y.; Nanayakkara, A.; Challacombe, M.; Gill, P. M. W.; Johnson, B.; Chen, W.; Wong, M. W.; Andres, J. L.; Gonzalez, C.; Head-Gordon, M.; Replogle, E. S.; Pople, J. A.; Piskorz, P.; Komaromi, I.; Gomperts, R.; Martin, R. L.; Fox, D. J. Gaussian 98, Revision A.11.2. **2001**. Pittsburgh PA, Gaussian, Inc.
[17] Portmann, S.; Luthi, H. P. *Chimia*, **2000**, *54*, 766.
[18] Jones, G.; Willet, P.; Glen, R. C.; Leach, A. R.; Taylor, R. *J. Mol. Biol*., **1997**, *267*, 727.
[19] Otake, Y.; Walle, T. *Drug Metab. Dispos*., **2002**, *30*, 103.
[20] Kuffel, M. J.; Schroeder, J. C.; Pobst, L. J.; Naylor, S.; Reid, J. M.; Kaufmann, S. H.; Ames, M. M. *Mol. Pharmacol.*, **2002**, *62*, 143.
[21] Brooks, B. R.; Bruccoleri, R. E.; Olafson, B. D.; States, D. J.; Swaminathan, S.; Karplus, M. J. *Comp. Chem*., **1983**, *4*, 187.
[22] Kollman, P. A.; Massova, I.; Reyes, C.; Kuhn, B.; Huo, S.; Chong, L.; Lee, M.; Lee, T.; Duan, Y.; Wang, W.; Donini, O.; Cieplak, P.; Srinivasan, J.; Case, D. A.; Cheatham, T. E. *Acc. Chem. Res*., **2000**, *33*, 889.
[23] Ramos, M. J.; Fernandes, P. A. *Curr. Comp-Aided Drug Des.*, **2004**, submitted.
[24] Rocchia, W.; Alexov, E.; Honig, B. *J. Phys. Chem. B*, **2001**, *105*, 6507.
[25] Sitkoff, D.; Sharp, K. A.; Honig, B. *J. Phys. Chem*., **1994**, *98*, 1978.
[26] Liu, J.; Ericksen, S. S.; Sivaneri, M.; Besspiata, D.; Fisher, C. W.; Szklarz, G. D. *Arch. Biochem. Biophys*., **2004**, *424*, 33.
[27] Parikh, A.; Josephy, P. D.; Guengerich, F. P. *Biochemistry*, **1999**, *38*, 5283.